Published OnlineFirst July 10, 2014; DOI: 10.1158/1078-0432.CCR-14-0259

Clinical Cancer Research

Cell and Molecular Determinants of *In Vivo* Efficacy of the BH3 Mimetic ABT-263 against Pediatric Acute Lymphoblastic Leukemia Xenografts

Santi Suryani, Hernan Carol, Triona Ni Chonghaile, et al.

Clin Cancer Res 2014;20:4520-4531. Published OnlineFirst July 10, 2014.

Published OnlineFirst July 10, 2014; DOI: 10.1158/1078-0432.CCR-14-0259

Personalized Medicine and Imaging

Clinical Cancer Research

Cell and Molecular Determinants of *In Vivo* Efficacy of the BH3 Mimetic ABT-263 against Pediatric Acute Lymphoblastic Leukemia Xenografts

Santi Suryani[1], Hernan Carol[1], Triona Ni Chonghaile[2], Viktoras Frismantas[3], Chintanu Sarmah[1], Laura High[1], Beat Bornhauser[3], Mark J. Cowley[4], Barbara Szymanska[1], Kathryn Evans[1], Ingrid Boehm[1], Elise Tonna[1], Luke Jones[1], Donya Moradi Manesh[1], Raushan T. Kurmasheva[5], Catherine Billups[6], Warren Kaplan[4], Anthony Letai[2], Jean-Pierre Bourquin[3], Peter J. Houghton[5], Malcolm A. Smith[7], and Richard B. Lock[1]

Abstract

Purpose: Predictive biomarkers are required to identify patients who may benefit from the use of BH3 mimetics such as ABT-263. This study investigated the efficacy of ABT-263 against a panel of patient-derived pediatric acute lymphoblastic leukemia (ALL) xenografts and utilized cell and molecular approaches to identify biomarkers that predict *in vivo* ABT-263 sensitivity.

Experimental Design: The *in vivo* efficacy of ABT-263 was tested against a panel of 31 patient-derived ALL xenografts composed of MLL-, BCP-, and T-ALL subtypes. Basal gene expression profiles of ALL xenografts were analyzed and confirmed by quantitative RT-PCR, protein expression and BH3 profiling. An *in vitro* coculture assay with immortalized human mesenchymal cells was utilized to build a predictive model of *in vivo* ABT-263 sensitivity.

Results: ABT-263 demonstrated impressive activity against pediatric ALL xenografts, with 19 of 31 achieving objective responses. Among *BCL2* family members, *in vivo* ABT-263 sensitivity correlated best with low *MCL1* mRNA expression levels. BH3 profiling revealed that resistance to ABT-263 correlated with mitochondrial priming by NOXA peptide, suggesting a functional role for MCL1 protein. Using an *in vitro* coculture assay, a predictive model of *in vivo* ABT-263 sensitivity was built. Testing this model against 11 xenografts predicted *in vivo* ABT-263 responses with high sensitivity (50%) and specificity (100%).

Conclusion: These results highlight the *in vivo* efficacy of ABT-263 against a broad range of pediatric ALL subtypes and shows that a combination of *in vitro* functional assays can be used to predict its *in vivo* efficacy. *Clin Cancer Res; 20(17); 4520–31. ©2014 AACR.*

Introduction

Despite significant improvements in the treatment of childhood acute lymphoblastic leukemia (ALL) over the past 5 decades, curing those patients who relapse with this most common pediatric malignancy remains a significant challenge (1). These relapse cases are often associated with broad-range drug resistance (2), which remains a significant problem, thus highlighting the need to develop new therapies. Because evasion of apoptosis is recognized as one of the hallmarks of cancer (3), recent drug development has focused on targeting key components of the apoptosis signaling pathway (4). The BCL2 family of proteins includes key regulators of the intrinsic apoptosis pathway, with cell fate being determined by the balance of prosurvival (e.g., BCL2 and MCL1) and proapoptotic (e.g., PUMA, NOXA) members (5, 6).

BH3-mimetic drugs, such as ABT-737 and its orally available analog ABT-263, were specifically designed to inhibit prosurvival BCL2 family proteins (7). Although these drugs bind with high affinity to BCL2, BCLW, and BCLXL, they exhibit lower affinity for MCL1 and A1 (7, 8). ABT-737 and ABT-263 have shown significant *in vivo* efficacy in preclinical xenograft models of hematolymphoid and solid malignancies (9, 10). Although clinical trials of ABT-263 in adults

[1]Children's Cancer Institute Australia for Medical Research, Lowy Cancer Research Centre, UNSW, Sydney, Australia. [2]Department of Medical Oncology, Dana-Farber Cancer Institute, Boston, Massachusetts. [3]Division of Pediatric Oncology, University Children's Hospital, Zurich, Switzerland. [4]Peter Wills Bioinformatics Centre, Garvan Institute of Medical Research, Darlinghurst, Australia. [5]Center for Childhood Cancer, Nationwide Children's Hospital, Columbus, Ohio. [6]Department of Biostatistics, St. Jude Children's Research Hospital, Memphis, Tennessee. [7]Cancer Therapy Evaluation Program, NCI, Bethesda, Maryland.

Note: Supplementary data for this article are available at Clinical Cancer Research Online (http://clincancerres.aacrjournals.org/).

S. Suryani and H. Carol contributed equally to this article.

Corresponding Author: Richard B. Lock, Children's Cancer Institute Australia for Medical Research, Lowy Cancer Research Centre, UNSW, P.O. Box 81, Randwick NSW 2031, Australia. Phone: 1800-685-686; Fax: 61-2-9662-6583; E-mail: rlock@ccia.unsw.edu.au

doi: 10.1158/1078-0432.CCR-14-0259

Published OnlineFirst July 10, 2014; DOI: 10.1158/1078-0432.CCR-14-0259

Translational Relevance

Manipulation of the apoptosis pathway is an appealing strategy for cancer treatment using BH3 mimetics such as ABT-263, although predictive biomarkers are required to identify patients who may benefit from their use. This study showed that ABT-263 exhibited broad *in vivo* efficacy against preclinical xenograft models of pediatric acute lymphoblastic leukemia (ALL). High *MCL1* expression, at the mRNA and protein level, correlated with *in vivo* ABT-263 resistance, which was confirmed functionally by BH3 profiling. In addition, *in vitro* coculture assays predicted *in vivo* ABT-263 responses with high sensitivity and specificity. Therefore, a combination of functional assays could be used to predict ABT-263 activity *in vivo*. Given the strong efficacy of ABT-263 against a significant proportion of xenografts tested, these in-principle approaches could be included in the design of prospective clinical trials to determine if they can identify patients who may respond to treatment with this class of therapeutic agents.

have shown promising results (11–13), the main dose-limiting toxicity of thrombocytopenia has hindered its progression into pediatric patients.

Consistent with the low affinity of ABT-737 and ABT-263 for MCL1, several reports have shown an inverse correlation of MCL1 expression with sensitivity to these drugs (14–16). Other proteins in the BCL2 family have also been implicated in determining sensitivity or resistance. For example, high BCL2 expression was associated with increased ABT-737 sensitivity in Non-Hodgkin's lymphoma (NHL) cell lines and in murine fetal liver cells (15). However, recent studies provided evidence that MCL1 or prosurvival protein expression levels contribute to, but are not sufficient determinants of, resistance (17–20). Disruption of the interaction between MCL1 and BAK increased drug sensitivity (17, 18), suggesting that protein–protein interactions, rather than absolute levels, play a critical role in determining the sensitivity to BH3 mimetics. This interpretation was reinforced by "mitochondrial BH3 profiling," which utilizes a panel of peptides derived from BH3-domains and their binding to antiapoptotic proteins, to predict a cell's susceptibility to apoptosis induction (19, 20). Mitochondrial sensitivity to the BAD BH3 peptide, which has a pattern of interaction with antiapoptotic proteins similar to ABT-737 and ABT-263, was shown to predict *in vitro* ABT-737 sensitivity in small cell lung cancer, lymphoma, ALL, and acute myelogenous leukemia cell lines (19). Clinical responses to conventional chemotherapy in acute leukemia, multiple myeloma, and ovarian cancer instead were found to correlate with mitochondrial sensitivity with promiscuous interacting BH3 peptides such as Puma BH3 (20).

The Pediatric Preclinical Testing Program previously reported that ABT-263 was effective as a single agent against *in vivo* models of childhood cancer, and in particular pediatric ALL xenografts (10). The results suggested preferential efficacy against 2 T-cell ALL (T-ALL) in comparison to B-cell precursor (BCP)-ALL xenografts, albeit testing against a small panel of xenografts. In this study, we tested the *in vivo* efficacy of ABT-263 against a diverse panel of 31 molecularly characterized xenografts derived from T-ALL, BCP-ALL, and infant ALL with translocations of the mixed lineage leukemia (*MLL*) gene (infant MLL-ALL), as well as the efficacy of ABT-263 in combination with established drugs. To identify determinants of *in vivo* ABT-263 response, we then correlated gene expression profiles, mitochondrial BH3 profiling and *in vitro* ABT-263 sensitivity with single-agent ABT-263 efficacy. This powerful approach can be used as proof-of-principle to identify determinants of *in vivo* responses to other novel antileukemic drugs.

Materials and Methods

Xenografts and *in vivo* drug treatments

All experimental studies were conducted with approval from the Animal Care and Ethics Committee of the University of New South Wales (Sydney, Australia). Procedures by which we established continuous xenografts from childhood ALL biopsies in immune-deficient NOD/SCID (NOD.CB17-Prkdc^{scid}/SzJ) or NOD/SCID, IL2 receptor γ negative (NOD.Cg-Prkdc^{scid} Il2rg^{tm1Wjl}/SzJ, NSG) mice, and tested their *in vivo* ABT-263 responses, have been described in detail previously (10, 21, 22). ALL subtypes were categorized at biopsy by their immunophenotype. Xenografts are available from the corresponding author upon request. ABT-263 (obtained from AbbVie under a standard Material Transfer Agreement) was administered orally at a dose of 100 mg/kg, daily for 21 days, as previously described (10). ABT-263 was also administered in combination with the conventional chemotherapeutic drugs vincristine (Baxter Healthcare; 1 mg/kg, days 0 and 7), dexamethasone (Sigma-Aldrich; 15 mg/kg, Mon–Fri × 2 weeks) or L-asparaginase (Aventis; 1,500 U/kg, Mon-Fri × 2 weeks) on a Mon to Fri × 2-week schedule at least 1 hour after administration of the established drug. It was necessary to attenuate the dose of ABT-263 to 25 mg/kg when combined with vincristine, and to 50 mg/kg when combined with dexamethasone and L-asparaginase in order to achieve a tolerable dose.

Leukemia engraftment and progression were assessed in groups of 6 to 10 female mice each of 20 to 25 g by weekly enumeration of the proportion of human CD45$^+$ cells in the peripheral blood (%huCD45$^+$; ref. 22). Individual mouse event-free survival (EFS) was calculated as the days from treatment initiation until the %huCD45$^+$ reached 25%. EFS was represented graphically by Kaplan–Meier analysis. The efficacy of drug treatment was evaluated by leukemia growth delay (LGD), calculated as the difference between the median EFS of vehicle control and drug-treated cohorts, as well as an objective response measure (ORM), modeled after stringent clinical criteria as described previously (21). Detailed methodology is presented in the Supplementary Methods and Table S1. Responses were also

Published OnlineFirst July 10, 2014; DOI: 10.1158/1078-0432.CCR-14-0259

expressed in a "COMPARE-like" format, which combines EFS and ORMs around the midpoint (0) representative of SD. Bars to the right or left of the midpoint represent objective responses or nonobjective responses, respectively. Significant and nonsignificant differences in EFS distribution between control and treated cohorts are represented by solid or dotted bars, respectively. Xenografts were excluded from analysis if >25% of mice within a cohort experienced nonleukemia-related toxicity or morbidity. Mice were excluded from the study if they developed spontaneous murine lymphomas.

To evaluate interactions between drugs *in vivo*, therapeutic enhancement was considered if the EFS of mice treated with the drug combination was significantly greater than those induced by both single agents used at their maximum tolerated doses (23, 24).

Protein expression

Preparation of extracts from xenograft cells previously harvested from the spleens of engrafted mice, determination of protein concentrations, and analysis of cellular proteins by immunoblotting have been described in detail elsewhere (25). Membranes were probed with anti-MCL1 (Genesearch) and anti-actin antibodies (Sigma-Aldrich) followed by horseradish peroxidase (HRP)—conjugated secondary antibody (GE Healthcare). Signal was detected by Immobilon Western Chemiluminescent HRP Substrate (Merck Millipore) and visualized using a VersaDoc 5000 Imaging System (Bio-Rad). Data were analyzed with QuantityOne software (Version 4.00; Bio-Rad).

RNA extraction, real-time quantitative reverse transcription PCR and gene expression analysis

Total RNA was extracted from xenograft cells, previously harvested from the spleens of engrafted mice and cryopreserved, using a combination of TRizol (Invitrogen) and Qiagen RNeasy Kit. RNA was purified with QIAGEN RNeasy spin columns, according to the manufacturer's protocol. RNA purity was considered acceptable if the ratio of $OD_{260/280}$ was between 1.8 and 2.0. For use in microarrays, the RNA integrity number was determined using an Agilent Bioanalyzer and considered acceptable if >7.

Real-time quantitative reverse transcription PCR (RT-qPCR) was carried out using standard techniques. First-strand cDNA was synthesized using 2 μg of total RNA, random primers (Roche), and M-MLV Reverse Transcriptase (Invitrogen). Primers and probes for *MCL1* were purchased from Life Technologies (Hs03043899_m1). Quantitative real-time PCR analysis was carried out in triplicate under the following cycling conditions: 50°C for 2 minutes and 95°C for 10 minutes, followed by 40 cycles of 95°C for 15 seconds and 60°C for 1 minute. Elongation factor-1α (*EF1α*) was used as an internal normalization standard in each reaction (primers EF1αF, 5′-CTGAACCATCCAGGCCAAAT-3′; EF1αR, 5′-GCCGTGTGGCAATCCAAT-3′; probe, 5′-VIC-AGCGCCGGCTATGCCCCTG-TAMRA-3′).

RNA samples were used to prepare cRNA with Illumina TotalPrep RNA Amplification Kit (Life Technologies). cRNA was then hybridized to Illumina Human Beadchip HT12 Arrays. Gene expression datasets were analyzed using GenePattern v3.2.3 as we have previously described (26). Gene expression datasets can be accessed at www.ncbi.nlm.nih.gov/geo (Accession No. GSE52991; reviewer's access: http://www.ncbi.nlm.nih.gov/geo/query/acc.cgi?token=glwjgwusrnadfsr&acc=GSE52991). Benjamini and Hochberg false discovery rate (FDR; ref. 27) measurement and Smyth unadjusted *P* value (28) were used for evaluation of differential gene expression. Gene expression heatmaps were generated using GenePattern, whereby the range of color coding extends from minimum to maximum values per gene (per row). In each case, red indicates high, and blue low, level of expression. Unsupervised hierarchical clustering was performed using the Hierarchical Clustering module in GenePattern using the entire 47,323 probes representative of 34,694 genes present in the Illumina Human Beadchip HT-12 Arrays.

Assessment of mitochondrial priming by BH3 profiling

Xenograft cells permeabilized by digitonin were exposed to BH3 peptides derived from BAD, NOXA, and PUMA proteins, and mitochondrial depolarization measured using the fluorescent dye JC-1, as we have previously described (20). Comparison of mitochondrial depolarization of nonresponders versus responders was performed using a *t* test (unpaired, 2-tailed).

In vitro cytotoxicity assays

The *in vitro* sensitivity of xenograft cells to ABT-263 was assessed by coculture using *hTERT*-immortalized primary bone marrow mesenchymal stromal cells (hTERT-MSC), as described previously (29) and detailed in the Supplementary Methods. Briefly, hTERT-MSCs were seeded at 2,000 cells/well in a 384-well plate (Greiner) in serum-free medium (AIM-V; Life Technologies). After 24 hours, 20,000 viable leukemia cells and ABT-263 were added to final concentrations of 1, 2.5, 5, 10, 25, 50, 100 and 1,000 nmol/L in duplicate. After 72 hours of incubation live-cell numbers were determined using 7-AAD analyses by flow cytometry (BD FACSCantoII). Data were normalized using SPHERO AccuCount Particles. Examples of flow cytometry analysis are included in Supplementary Fig. S1. To build a predictive model of *in vivo* ABT-263 sensitivity, we used upper and lower limits of the 95% confidence intervals of the proportion of live cells after exposure to 10 nmol/L of ABT-263 *in vitro*.

Statistical analysis

EFS curves were compared by the log-rank test. Differences in responses to single-agent ABT-263 *in vivo* between MLL-ALL, BCP-ALL, and T-ALL xenografts were evaluated using one-way ANOVA and a Tukey multiple comparison analysis as well as χ^2 test. A Pearson correlation test was utilized for all datasets with normal distribution, which included gene expression analysis versus LGD, and *MCL1* Illumina mRNA versus *MCL1* RT-qPCR mRNA levels. A Spearman correlation test was used to compare *MCL1*

Published OnlineFirst July 10, 2014; DOI: 10.1158/1078-0432.CCR-14-0259

RT-qPCR mRNA versus protein expression. Comparison of *MCL1* RT-qPCR mRNA and protein levels between non-responders and responders was performed using a Mann–Whitney test. Significance was inferred from tests with *P* values lower than 0.05.

Results

Gene expression profiles of ALL xenografts reflect the primary disease

To identify cell and molecular determinants of *in vivo* ABT-263 responses in pediatric ALL, panels of a total of 31 xenografts were established from direct patient explants representative of MLL-ALL (8 infant MLL-ALLs and 1 pediatric MLL-ALL, ALL-3), BCP-ALL ($n = 7$), and T-ALL ($n = 15$) and were characterized by gene expression profiling. The patient demographics focused on high-risk or poor outcome cases: infant MLL-ALL is a known high-risk ALL subtype; the T-ALL panel included 3 xenografts derived from patients with early T-cell precursor (ETP) ALL (ETP-1, ETP-2, and ETP-3), a very high-risk subgroup (30); the BCP-ALL and non-ETP T-ALL panels included 4 of 7 and 9 of 12 patients, respectively, who had relapsed and/or died from their disease (22, 30, 31). More detailed descriptions of the infant MLL-ALL and expanded T-ALL xenograft panels will be reported elsewhere. Chromosomal translocations in the original biopsy sample, where known, are summarized in Supplementary Table S2.

Unsupervised hierarchical clustering of xenograft basal gene expression profiles revealed 3 distinct branches reflecting each leukemia subtype (Fig. 1A). The MLL-ALL and BCP-ALL panels seemed more closely related and distinct from the T-ALL xenografts. Xenograft ALL-3 was originally classified by immunophenotype as a BCP-ALL but clustered with the MLL-ALLs. Upon further investigation it was confirmed that ALL-3 harbors an *MLL* gene rearrangement (Supplementary Table S2). The 4 MLL-ALLs with translocations involving chromosome 19 (MLL-6, MLL-8, MLL-14, and ALL-3) clustered separately from 2 MLL-ALLs with chromosome 4 translocations (MLL-2 and MLL-7; Fig. 1A and Supplementary Table S2). The 3 ETP-ALLs, while not clustering as a separate branch, did cluster within the T-ALL panel (Fig. 1A).

We next identified subtype-specific differentially expressed genes using the LimmaGP (Cowley and colleagues, manuscript in preparation) module in GenePattern, whereby each subtype was compared with the remaining 2 ALL subtypes (1 vs. rest comparison). Subtype-specific genes were determined with a cut-off value of FDR < 0.05. At this level of stringency, there were 2,141 MLL-ALL specific genes, 643 BCP-ALL specific genes, and 18,692 T-ALL specific genes (Supplementary Table S3). The top 25 differentially expressed probesets between each xenograft panel included previously identified subtype-specific genes, such as *MEIS1*, *ZNF827*, and *CCNA1* in MLL-ALL (32), *MME* (CD10) in BCP-ALL, and components of the CD3 receptor (*CD3D*, *CD3E*, *CD3G*, and *CD247*), *CD2* and *SH2D1A* in T-ALL (ref. 33; Fig. 1B). ALL subtype-specific genesets were identified using GSEA preranked module in GenePattern with FDR < 0.05 (Supplementary Table S4). For MLL-ALL, the top 4 genesets reflected MLL-specific genesets, for BCP-ALL, 9 B-cell–specific genesets were identified within the top 30 genesets and for T-ALL, 6 T-cell–specific genesets were identified within the top 10 genesets. Therefore, these analyses confirmed the xenograft subtype classification according to the primary disease.

ABT-263 exhibits single-agent *in vivo* efficacy against a broad range of pediatric ALL subtypes

We previously reported the results of *in vivo* ABT-263 testing against a panel of 6 ALL xenografts, with higher sensitivity observed in 2 T-ALL compared with 4 BCP-ALL xenografts (10). To further investigate this possible subtype-specific *in vivo* efficacy of ABT-263 against pediatric ALL, we expanded the analysis to the 31 xenografts described above. ABT-263 significantly delayed the progression of 29 of 31 xenografts tested (Table 1, Fig. 2A–C, and Supplementary Figs. S2–S4). LGDs ranged from 0.5 (ALL-2; $P = 0.46$) to 78 (ALL-31; $P = 0.0008$) days. When stratified according to ALL subtype the median LGDs were 17.9 days for MLL (range 3.1–53.7), 25.8 days for BCP-ALL (range 0.5–37.9), and 29.6 days for T-ALL (range 4.0–78; Fig. 2D and Table 1). There was no significant differential efficacy of ABT-263 against any of the 3 ALL subtypes.

ABT-263 elicited objective responses in 19 of 31 xenografts, with 3 MCRs, 11 CRs, and 5 PRs (Table 1 and Fig. 2). Figure 2E represents the *in vivo* ABT-263 responses of each xenograft panel in a "COMPARE-like" format. In agreement with the LGD data, no significant differences were observed between the ALL subtypes.

We previously showed that the *in vivo* sensitivity of a subset of these xenografts to an induction-type regiment of vincristine, dexamethasone, and L-asparaginase (VXL) correlated with the clinical outcome of the patients from whom the xenografts were derived (34). However, the *in vivo* ABT-263 sensitivity of the same subset of xenografts did not correlate with their VXL responses ($R = 0.46$, $P = 0.18$; Supplementary Fig. S5), indicating that ABT-263 can exert significant *in vivo* efficacy against ALL xenografts that are resistant to established drugs.

A complete summary of results is provided in Supplementary Figs. S2 to S4 and Table S5, including total numbers of mice, number of mice that died (or were otherwise excluded), numbers of mice with events and average times to events, LGD values, as well as numbers in each of the ORM categories and "treated over controls" (*T*/*C*) values.

MCL1 gene expression correlates with *in vivo* ABT-263 sensitivity in ALL xenografts

We next analyzed basal *BCL2* family gene expression levels in relation to *in vivo* ABT-263 sensitivity across the 31 xenografts using 2 approaches. Both approaches were applied to the entire xenograft cohort as well as all 3 subtypes separately. The first approach assessed the correlation between gene expression and progression delay (LGD; Pearson product moment correlation coefficient), with a positive correlation denoting genes whose higher

Published OnlineFirst July 10, 2014; DOI: 10.1158/1078-0432.CCR-14-0259

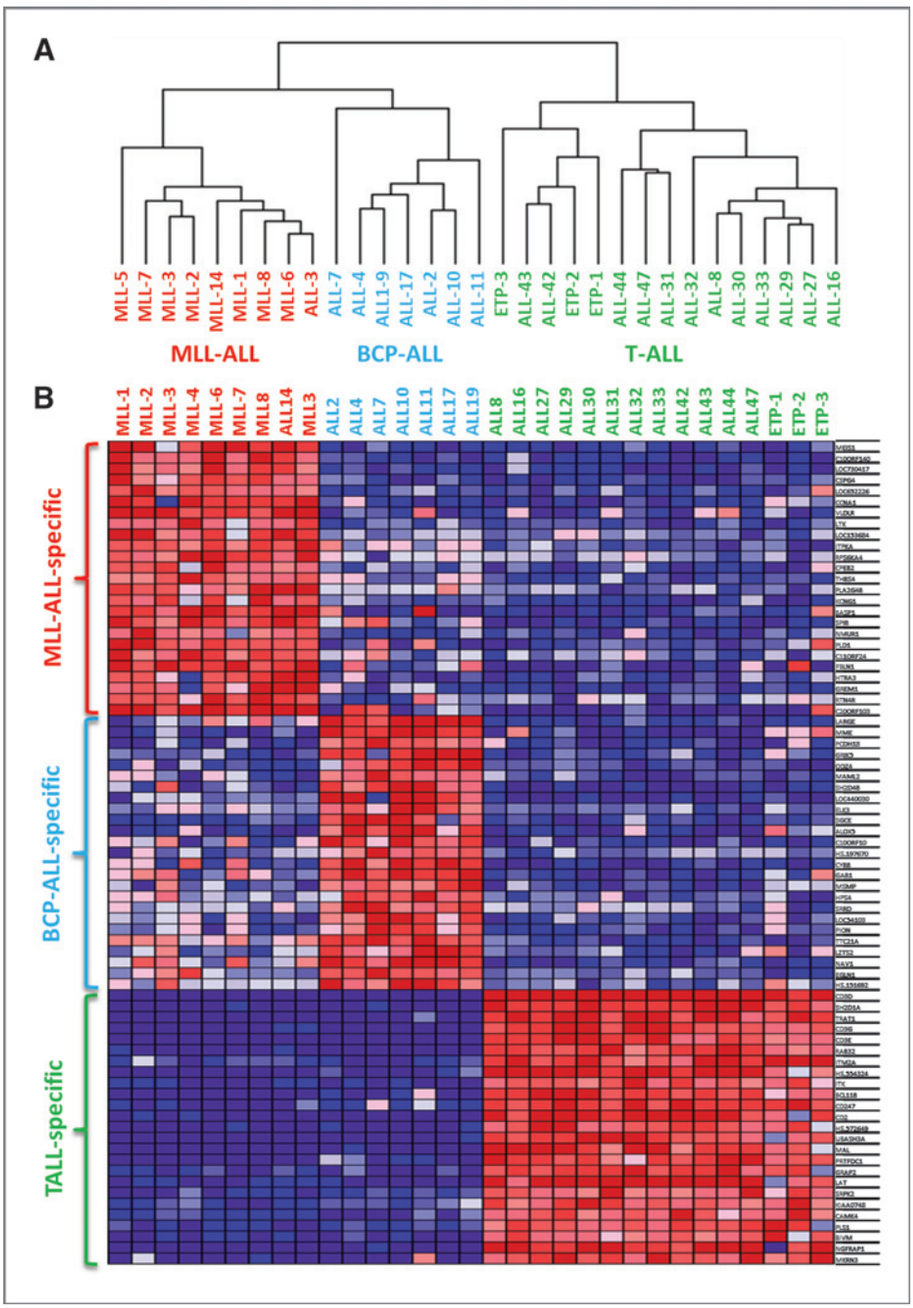

Figure 1. Comparison of MLL-ALL, BCP-ALL, and T-ALL xenografts by gene expression profiling. A total of 31 ALL xenografts (MLL-ALL, $n = 9$; BCP-ALL, $n = 7$; T-ALL, $n = 15$) were profiled on Illumina Human HT-12 Beadchip arrays. A, nonsupervised hierarchical clustering of all xenografts. B, heatmap of the top 25 upregulated genes that were specific to MLL-ALL, BCP-ALL, and T-ALL subtypes ordered according to their *P* value. The colors in the heatmaps represent the relative expression per gene across all samples. Red indicates relative high expression and blue indicates relative low expression.

expression was associated with ABT-263 sensitivity, and *vice versa*. Using this approach, *MCL1* expression correlated significantly with *in vivo* ABT-263 sensitivity across the entire xenograft panel ($R = -0.43$, $P = 0.015$; Fig. 3A), indicating that high *MCL1* expression was associated with *in vivo* resistance. *BCLXL/XS* ($R = 0.79$, $P = 0.01$) and *BCLW* ($R = 0.69$, $P = 0.039$) showed significant positive correlations between expression and drug sensitivity in the MLL-ALL panel (Supplementary Fig. S6 and Table S6). In contrast, no significant correlations were observed in the BCP-ALL panel (Supplementary Fig. S7 and Table S6) whereas *BID* levels were negatively correlated with sensitivity in the T-ALL xenografts ($R = -0.52$, $P = 0.046$; Supplementary Fig. S8 and Table S6).

In the second approach, xenografts were stratified according to their ORM into responders (PRs, CRs, and MCRs) and nonresponders (PDs and SDs) and differentially expressed genes were identified using an unadjusted *P* value of ≤ 0.05 from an empirical Bayes moderated *t* test (28). *MCL1* was the *BCL2* family member with the strongest differential expression among the entire xenograft panel between responders and nonresponders (Fig. 3B and Supplementary Table S6). This was also the case for the MLL-ALL ($P = 0.027$) and BCP-ALL ($P = 0.008$) subtypes (Supplementary

Published OnlineFirst July 10, 2014; DOI: 10.1158/1078-0432.CCR-14-0259

Table 1. *In vivo* responses of pediatric ALL xenografts to ABT-263

		EFS (days)					
ALL lineage	**Xenograft ID**	**Vehicle control**	**ABT-263**	**LGD (days)**	***P* value (log-rank)**	**Median ORM**	**ORM heatmap**
MLL-ALL	MLL-1	19.2	39.7	20.5	0.0003	6	PR
	MLL-2	14.8	26.8	12.0	0.002	6	PR
	MLL-3	8.3	34.1	25.8	0.0002	8	CR
	MLL-5	8.7	14.6	5.9	0.0006	2	PD2
	MLL-6	6.3	29.1	22.8	0.0002	2	PD2
	MLL-7	12.7	30.6	17.9	0.0002	6	PR
	MLL-8	13.7	16.8	3.1	0.0002	0	PD1
	MLL-14	8.7	24.9	16.2	0.0006	2	PD2
	ALL-3	9.6	63.3	53.7	0.008	8	CR
BCP-ALL	ALL-2[a]	4.7	5.2	0.5	0.46	0	PD1
	ALL-4[a]	1.5	28.6	27.1	0.029	2	PD2
	ALL-7	6.8	31.4	24.6	0.0003	8	CR
	ALL-10	7.5	33.3	25.8	0.008	8	CR
	ALL-11	20.2	56.3	36.1	0.008	8	CR
	ALL-17[a]	2.5	24.2	21.7	0.0001	2	PD2
	ALL-19[a]	5.0	>43	>37.9	0.002	8	CR
T-ALL	ALL-8[a]	11.8	62.8	51.0	0.004	10	MCR
	ALL-16[a]	18.2	85.5	67.3	0.0002	10	MCR
	ALL-27	3.3	19.6	16.3	0.30	2	PD2
	ALL-29	4.4	48.8	44.0	0.0002	8	CR
	ALL-30	5.3	16.2	10.9	0.004	2	PD2
	ALL-31	13.9	91.9	78.0	0.0008	10	MCR
	ALL-32[b]	6.7	18.9	12.2	0.0002	2	PD2
	ALL-33[b]	6.0	37.8	31.8	0.0003	8	CR
	ALL-42	1.9	5.9	4.0	0.0002	2	PD2
	ALL-43	14.0	43.9	29.9	0.0002	8	CR
	ALL-44	11.4	27.2	15.8	0.0005	2	PD2
	ALL-47	11.9	41.5	29.6	<0.0001	8	CR
ETP-ALL	ETP-1	7.8	23.8	16.0	0.0002	6	PR
	ETP-2	14.2	44.7	30.5	0.0002	8	CR
	ETP-3	20.0	32.5	12.5	0.0002	6	PR

[a]*In vivo* ABT-263 sensitivity data previously reported (10).

[b]Dose of ABT-263 reduced to 75 mg/kg on day 9 (ALL-32) or day 13 (ALL-33) because of toxicity.

Figs. S6 and S7 and Table S6). Among the MLL-ALL xenografts, differential expression of *BIM* ($P = 0.044$); also reached statistical significance, being paradoxically lower in the responders compared with nonresponders (Supplementary Fig. S6 and Table S6). Similarly, *HRK* ($P = 0.005$) was significantly increased in the BCP-ALL responders (Supplementary Fig. S7 and Table S6), whereas *BAK* ($P = 0.03$) and *NOXA* ($P = 0.049$) were significantly increased in the T-ALL nonresponders and responders, respectively (Supplementary Fig. S8 and Table S6).

Both of the above analysis approaches had also been applied to the entire 34,694 genes represented on the Illumina Beadchip HT-12 arrays, although no genes satisfied the significance or FDR cutoff criteria (data not shown).

Because *MCL1* expression was the strongest overall predictor of *in vivo* ABT-263 response across the entire panel of 31 xenografts, we next assessed *MCL1* expression at the mRNA and protein levels. Although RT-qPCR analysis showed a significantly higher *MCL1* expression in the nonresponders (Fig. 3C), this difference was not confirmed by increased MCL1 protein levels (Fig. 3D and Supplementary Fig. S9). Despite no significant difference in MCL1 protein levels between non-responders and responders, *MCL1* mRNA levels correlated between qRT-PCR and microarray (Fig. 3E), and MCL1 protein levels significantly correlated with *MCL1* mRNA expression measured by qRT-PCR (Fig. 3F). MCL1 protein expression was also investigated after exposure of 2 non-responders and 2 responders to ABT-263 *in vitro*, however no consistent differences were observed (data not shown). Because of these discrepancies in MCL1 protein expression, we next assessed BCL2 family protein

Published OnlineFirst July 10, 2014; DOI: 10.1158/1078-0432.CCR-14-0259

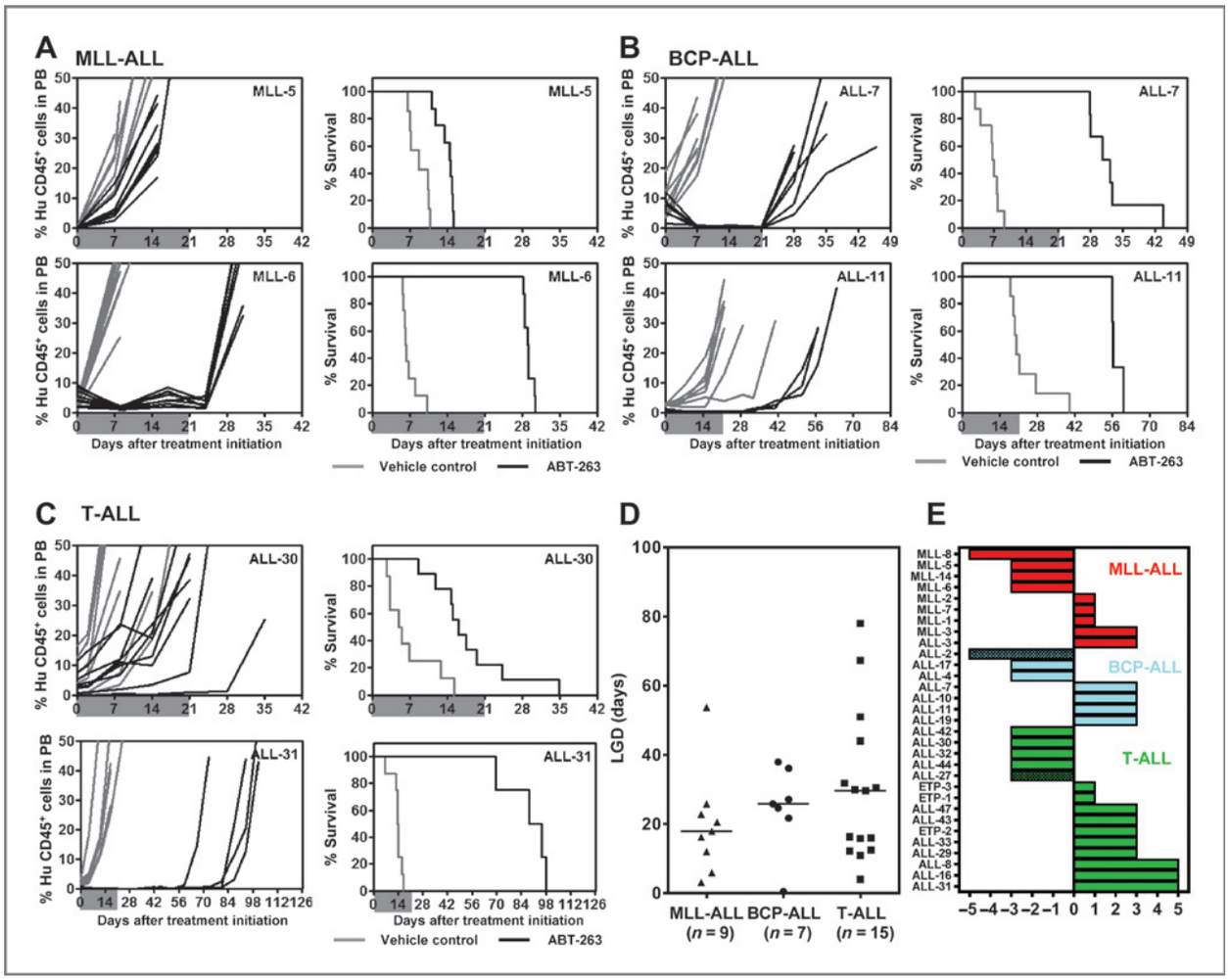

Figure 2. *In vivo* single-agent ABT-263 responses of pediatric ALL xenografts. Responses of representative xenografts from the MLL-ALL (A), BCP-ALL (B), and T-ALL (C) subpanels treated with ABT-263 (100 mg/kg for 21 days, black lines) or vehicle control (gray lines). In each case, the left panels represent the %huCD45$^+$ of individual mice over time, whereas the right panels represent the proportion of mice remaining event free. Shaded areas indicate the treatment period. D, comparison of the LGD of ALL xenograft subtypes in response to ABT-263 treatment. Each data point represents a single xenograft; the horizontal bar represents the median. E, "COMPARE-like" plot of the midpoint difference representing the median ORM of xenografts shown in Table 1.

function with respect to *in vivo* ABT-263 sensitivity using BH3 profiling of the entire xenograft panel.

BH3 profiling identifies MCL1 function as a determinant of *in vivo* ABT-263 sensitivity

The mitochondrial priming assay measures mitochondrial sensitivity to peptides derived from the BH3 domains of proapoptotic BCL2 family proteins. The *in vivo* ABT-263 responses of the xenografts were then compared with the status of mitochondrial priming by the ability of BH3 peptides derived from PUMA, BAD, and NOXA to cause mitochondrial depolarization in xenograft cells. PUMA BH3 interacts promiscuously with all 5 antiapoptotic proteins, BAD BH3 interacts with BCL2, BCLXL, and BCLW (like ABT-263), whereas NOXA BH3 interacts only with MCL1. Out of the 3 peptides, only NOXA-induced mitochondrial depolarization significantly discriminated between non-responder and responder groups (Fig. 3G–I), implicating MCL1 protein function as a major determinant of *in vivo* ABT-263 response. The extent of mitochondrial depolarization did not correlate with leukemia progression (LGD) for any of the peptides tested (data not shown).

In vitro ABT-263 sensitivity of ALL xenografts predicts their *in vivo* responses

We next tested whether the *in vitro* ABT-263 responses of ALL xenografts predicted their *in vivo* sensitivity. Using a coculture method (29), a predictive model was built using a training subset of 17 xenografts (Fig. 4A). Exposure of xenograft cells to a range of ABT-263 concentrations (1 μmol/L–1 nmol/L) revealed that 10 nmol/L gave the best discrimination between *in vivo* non-responders and responders (Fig. 4B and Supplementary Fig. S10). Using the 95%

Published OnlineFirst July 10, 2014; DOI: 10.1158/1078-0432.CCR-14-0259

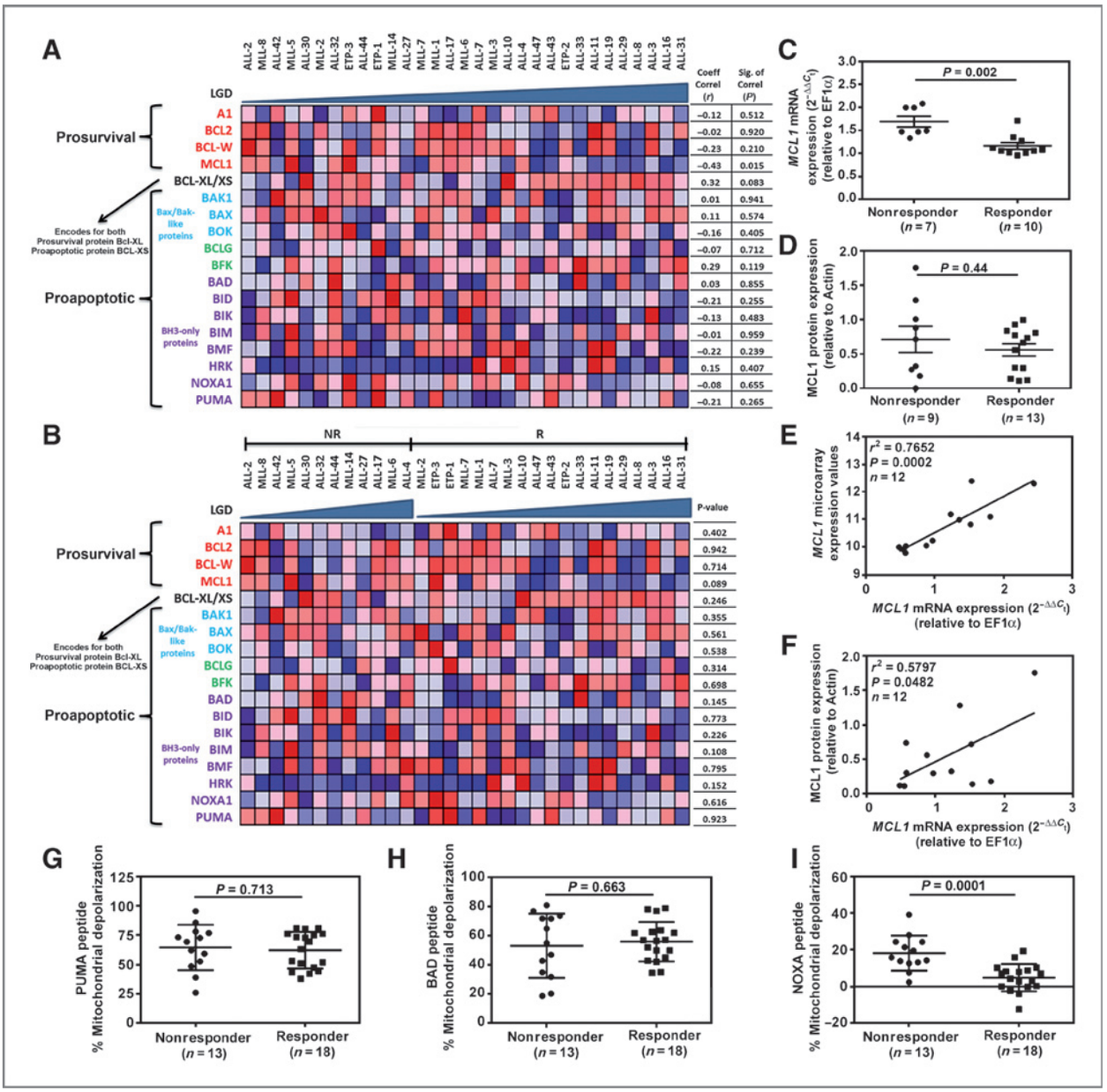

Figure 3. Cell and molecular determinants of the *in vivo* sensitivity of pediatric ALL xenografts to ABT-263. A, xenografts (columns) were ordered by increasing LGD from left to right, with each row representing a *BCL2* family member. B, xenografts were stratified into nonresponders (NR) and responders (R) then ordered by increasing LGD from left to right within each category. The colors in the heatmaps represent the relative expression per gene across all samples. Red indicates relative high expression and blue indicates relative low expression. C, comparison of *MCL1* mRNA expression between NR and R by RT-qPCR. D, comparison of MCL1 protein expression between NR and R by immunoblot. E, correlation between *MCL1* mRNA expression by microarray and RT-qPCR. F, correlation between MCL1 protein expression by immunoblot and *MCL1* mRNA expression by RT-qPCR. In C–F, each data point represents a single xenograft. G–I, the percentage of mitochondrial depolarization induced by BH3 peptides derived from (G) PUMA, (H) BAD, and (I) NOXA peptides in xenograft cells was plotted for individual xenografts stratified as NR or R according to Table 1.

confidence intervals of both responder and nonresponder groups, a three-tier classification was created. It was established that >14.9% live cells after drug treatment (lower limit of confidence interval of nonresponders) stratified xenografts as nonresponders, <8.0% (upper limit of confidence interval of responders) as responders, and those in between were considered as unclassified. Three xenografts (MLL-1, MLL-7, and ETP-3) were excluded from the analysis because their survival was not supported by the coculture assay.

The *in vivo* ABT-263 responses of the remaining 11 xenografts, constituting the test set, were initially blinded. When the test set was classified using the predictive model 7 xenografts were correctly classified according to their *in vivo*

Published OnlineFirst July 10, 2014; DOI: 10.1158/1078-0432.CCR-14-0259

A

	Training set	Test set
In vivo nonresponder	ALL-2	ALL-17
	ALL-4	ALL-32
	ALL-27	ALL-44
	ALL-30	MLL-8
	ALL-42	MLL-14
	MLL-5	
	MLL-6	
In vivo responder	ALL-3	ALL-11
	ALL-8	ALL-16
	ALL-10	ALL-19
	ALL-7	ETP-1
	ALL-29	ALL-47
	ALL-31	MLL-3
	ALL-33	
	ETP-2	
	ALL-43	
	MLL-2	

B

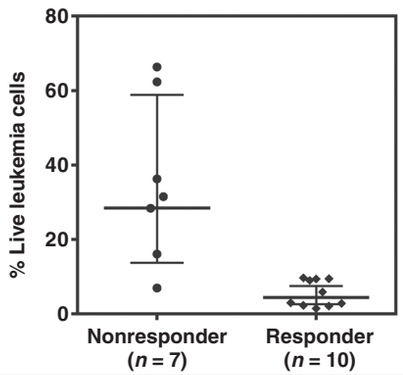

Nonresponder 95% lower confidence interval: 14.9%
Responder 95% upper confidence interval: 8.0%

C

	Test set	Prediction
In vivo non-responder	ALL-17	Nonresponder
	ALL-32	Nonresponder
	ALL-44	Nonresponder
	MLL-8	Nonresponder
	MLL-14	Nonresponder
In vivo responder	ALL-11	Nonresponder
	ALL-16	Unclassified
	ALL-19	Nonresponder
	ALL-37	Unclassified
	ALL-47	Responder
	MLL-3	Responder

Figure 4. *In vitro* sensitivity of pediatric ALL xenograft cells to ABT-263 predicts their *in vivo* responses. A, xenografts were subgrouped into a training set to build a predictive model, and a test set to test the model. B, percentages of live leukemia cells after exposure to ABT-263 (10 nmol/L, 72 hours). Each data point represents an individual xenograft. Lines indicate the geometric mean with 95% confidence interval indicated by the bars. C, actual and predicted *in vivo* ABT-263 responses of the test xenografts.

ABT-263 responses (Fig. 4C), 2 were incorrectly classified and 2 were unclassified. The sensitivity and specificity of the predictive method (Supplementary Fig. S11) were 50% and 100%, respectively (leaving out of this assessment the 2 unclassified xenografts).

Live and dead cell analysis at 72 hours for each xenograft is shown in Supplementary Fig. S12, which includes the % live/dead cells, the absolute numbers of live/dead cells, and the number of live cells seeded and harvested. In addition, a comparison of the coculture system versus single cell suspension was performed with 5 xenograft samples, and revealed the importance of the coculture assay to assess ALL xenograft cell sensitivity to ABT-263 *in vitro* (Supplementary Fig. S13).

In vivo efficacy of ABT-263 in combination with established chemotherapeutic drugs

We next sought to test the efficacy of ABT-263 in paired combinations with established drugs against xenografts representative of the 2 most common pediatric ALL subtypes, BCP-ALL and T-ALL. Three xenografts were selected based on their range of single-agent ABT-263 responses (ALL-2, resistant; ALL-19, intermediate; ALL-31, sensitive; Table 1). Preliminary tolerability experiments showed that it was necessary to attenuate the dose of ABT-263 to 25 mg/kg when combined with vincristine, and to 50 mg/kg when combined with dexamethasone and L-asparaginase. Of the 3 xenografts tested, the combination of ABT-263 with vincristine caused therapeutic enhancement only in ALL-31 and although for ALL-19 it induced an LGD of >73.7 days, because variation among individual mice it did not reach statistical significance versus ABT-263 alone (Supplementary Tables S7 and S8 and Fig. S14). The dexamethasone/ABT-263 combination did not exert therapeutic enhancement for any xenografts, whereas ABT-263 in combination with L-asparaginase exerted therapeutic enhancement in ALL-31, and the *P* value approached significance for ALL-19. Thus, the expectation that ABT-263 would broadly enhance the *in vivo* efficacy of established chemotherapeutic drugs was not met.

Discussion

We report the utilization of a large panel of ALL xenografts to define the cell and molecular determinants of *in vivo* ABT-263 responses using gene expression profiling, BH3 profiling, and *in vitro* coculture cytotoxicity assays. The principal findings of this study are: (i) ABT-263 is effective *in vivo* as a single agent against pediatric ALL xenografts; (ii) *MCL1*

Published OnlineFirst July 10, 2014; DOI: 10.1158/1078-0432.CCR-14-0259

gene expression and MCL1 protein function correlate with *in vivo* ABT-263 sensitivity; and (iii) an *in vitro* coculture cytotoxicity assay is able to predict *in vivo* ABT-263 responses of ALL xenografts with a high level of sensitivity and specificity.

Xenograft models of pediatric ALL are recognized to accurately recapitulate several cellular and molecular features of the original disease, including blast morphology, immunophenotype, clonal selection, gene expression profiles, and genetic lesions (22, 31, 35–37). Our results describe the subtype classification of a large panel of xenografts, which were appropriately clustered into MLL-ALL, BCP-, and T-ALL subtypes by gene expression profiling. Differentially expressed genes and GSEA analysis within each subtype were consistent with the primary disease state, and a BCP-ALL xenograft previously established from a teenage female (31) was reclassified as an MLL-ALL based in this analysis. Subclusters within each xenograft subtype were also consistent with specific chromosomal translocations. For example, all 4 of the MLL-ALL xenografts harboring a translocation involving chromosome 19 coclustered in 1 subbranch of MLL-ALL, whereas the 3 ETP-ALLs appeared under 1 subbranch of T-ALL.

Despite our previous report of ABT-263 efficacy testing against 6 ALL xenografts indicating a preferential effect against 2 T-ALL xenografts (10), in this study ABT-263 exhibited a broad spectrum of *in vivo* efficacy with no apparent subtype specificity, and induced regressions in 19 of 31 xenografts. However, all 3 xenografts that achieved MCRs were T-ALL, suggesting that ABT-263 may be particularly useful for the treatment of aggressive T-ALL cases. ABT-263 also induced regressions (2 PRs and 1 CR) in the 3 ETP-ALL xenografts. ETP-ALL arises from a subset of thymocytes that are recent emigrants from the bone marrow to the thymus, retaining stem cell–like features and multilineage differential potential, and is a particularly aggressive and refractory T-ALL subtype (30).

In this study, we also attempted to identify cell and molecular signatures that could be used to predict *in vivo* responsiveness to single-agent ABT-263. Studies primarily carried out using cultured cell lines have consistently identified elevated *MCL1* expression to be associated with resistance to ABT-737 and ABT-263 (14–16, 38). Although our study is no exception, we believe this to be the first report to strongly implicate *MCL1* in resistance to ABT-263 *in vivo* using a large panel of direct-patient explants established as continuous xenografts. This relationship only became apparent when we restricted the gene expression analysis to the *BCL2* gene family, a finding that we attribute to the heterogeneity in gene expression profiles between and within each xenograft subtype. Nevertheless, the molecular determinants of *in vivo* ABT-263 sensitivity in pediatric ALL are complex since additional, and occasionally paradoxically, *BCL2* family genes were significantly associated with ABT-263 responses within individual xenograft subtypes.

A confounding factor in our analysis was that, although *MCL1* mRNA expression determined by RT-qPCR correlated with MCL1 protein expression and microarray data, MCL1 protein expression did not reach statistical significance between the ABT-263 responders and non-responders despite a higher trend in the nonresponders (Fig. 3D). Technical issues associated with the harvesting, purifying, and cryopreservation of spleen-derived cells and the very short half-life of MCL1 (<1 hour; refs. 39 and 40) may have contributed to this lack of correlation because of MCL1 protein degradation (Supplementary Fig. S15). Moreover, Gao and Koide reported that there are 2 MCL1 splice variants regulated by *SF3B1*, one with proapoptotic and another with antiapoptotic functions (41). However, we found no correlation between *SF3B1* levels and drug sensitivity (data not shown). Similarly, Boiani and colleagues showed that the HSP70 protein BAG3 stabilizes MCL1, thereby extending its half-life (42). Similarly, we found no correlation between *BAG3* expression and *in vivo* ABT-263 efficacy (data not shown). Because of the aforementioned complexity associated with correlating gene expression profiles and MCL1 protein expression with *in vivo* ABT-263 sensitivity, we next tested the established functional readouts of mitochondrial priming status by BH3 profiling and *in vitro* chemosensitivity testing. Mitochondrial depolarization induced by NOXA peptide correlated with *in vivo* ABT-263 sensitivity (Fig. 3I), thereby strongly implicating MCL1 function. However, this finding differs from a previous report that identified a correlation between BIM, but not NOXA, peptide-induced mitochondrial depolarization and clinical complete response to conventional therapy using pediatric ALL biopsy samples (20).

Murine or human bone marrow–derived stromal cells improve the *ex vivo* survival of pediatric ALL cells (29, 43) whereas both coculture and tetrazolium dye-based assays have been used for chemosensitivity testing in this disease (44–46). In our study, ABT-263 sensitivity of pediatric ALL xenograft cells cocultured with MSC-hTERT cells provided a sensitive (50%) and highly specific (100%) prediction of *in vivo* response. This model accurately predicted resistance, because all 5 of the *in vivo* nonresponders were correctly identified. However, although both of the xenografts predicted to be responders were correct, the model incorrectly predicted no response in 2 of the *in vivo* responders. Therefore, this model could be further refined, because although it might accurately predict which patients are unlikely to respond, it can potentially fail to identify a subset of patients who may benefit from such treatment. Nevertheless, we believe this to be the first report of a functional assay that is able to accurately predict *in vivo* single-agent ABT-263 responses.

Despite substantial evidence, primarily using cultured cell lines, that ABT-737 and ABT-263 can potentiate the effects of standard chemotherapeutic drugs both *in vitro* and *in vivo* (9, 16, 47, 48), using stringent criteria we only observed Therapeutic Enhancement in 2 instances in which ABT-263 was combined with 3 established drugs against 3 xenografts. Although our results are not sufficient to make broad conclusions for combining ABT-263 with these established drugs for patient management, we reason that this divergence from previous reports is because of the necessity

Published OnlineFirst July 10, 2014; DOI: 10.1158/1078-0432.CCR-14-0259

to attenuate the ABT-263 dose in all of the combinations (down to 25 mg/kg in the case of vincristine), while maintaining the maximal ABT-263 dose (100 mg/kg) in the single-agent arms. Future investigations in which small-molecule BCL2 inhibitors with reduced thrombocytopenic effects, such as ABT-199 (49, 50), are combined with established drugs in pediatric ALL may prove more beneficial.

In summary, BCL2-targeted agents appear as a promising class of anticancer drugs for the treatment of pediatric ALL, with no apparent specificity across MLL-ALL, BCP-ALL, or T-ALL subtypes. *MCL1* expression and function seem to be important determinants of *in vivo* ABT-263 sensitivity, although an *in vitro* coculture assay predicted *in vivo* ABT-263 responses with high sensitivity and specificity. This combined cell and molecular analysis provides a proof-of-concept approach for prioritizing other novel drugs for pediatric ALL clinical trials, and for the identification of biomarkers predictive of *in vivo* response.

Disclosure of Potential Conflicts of Interest

Anthony Letai is a consultant/advisory board member for AbbVie. No potential conflicts of interest were disclosed by the other authors.

Authors' Contributions

Conception and design: H. Carol, C. Sarmah, P.J. Houghton, M.A. Smith, R.B. Lock

Development of methodology: H. Carol, T.N. Chonghaile, V. Frismantas, B. Bornhauser, A. Letai, J.-P. Bourquin, P.J. Houghton, M.A. Smith, R.B. Lock

Acquisition of data (provided animals, acquired and managed patients, provided facilities, etc.): S. Suryani, H. Carol, T.N. Chonghaile, V. Frismantas, L. High, B. Szymanska, K. Evans, I. Boehm, E. Tonna, L. Jones, D.M. Manesh, A. Letai, J.-P. Bourquin

Analysis and interpretation of data (e.g., statistical analysis, biostatistics, computational analysis): S. Suryani, H. Carol, T.N. Chonghaile, V. Frismantas, C. Sarmah, L. High, B. Bornhauser, M.J. Cowley, B. Szymanska, K. Evans, I. Boehm, E. Tonna, L. Jones, R.T. Kurmasheva, C. Billups, W. Kaplan, A. Letai, J.-P. Bourquin, P.J. Houghton, M.A. Smith, R.B. Lock

Writing, review, and/or revision of the manuscript: S. Suryani, H. Carol, C. Sarmah, B. Bornhauser, M.J. Cowley, B. Szymanska, K. Evans, E. Tonna, L. Jones, P.J. Houghton, M.A. Smith, R.B. Lock

Administrative, technical, or material support (i.e., reporting or organizing data, constructing databases): S. Suryani, K. Evans, E. Tonna, R.T. Kurmasheva

Study supervision: S. Suryani, H. Carol, R.B. Lock

Acknowledgments

The authors thank AbbVie Inc. for providing ABT-263, the Tissue Resources Core Facility of St Jude Children's Research Hospital (Memphis, TN) for the provision of primary ETP-ALL samples, and Dr Dario Campana (St Jude Children's Research Hospital, Memphis, TN) for providing *hTERT*-immortalized MSCs. Children's Cancer Institute Australia for Medical Research is affiliated with the University of New South Wales and The Sydney Children's Hospitals Network.

Grant Support

This research was funded by grants from the National Cancer Institute (NOI-CM-42216 and NOI-CM-91001-03); the Leukaemia Foundation of Australia the Cancer Council New South Wales; the Krebsliga Zurich to B. Bornhauser, and the Foundation Kind und Krebs, the Hanne Liebermann Stiftung, and the Swiss National Research Foundation to J.-P. Bourquin. S. Suryani is supported by Postdoctoral Fellowships from the Leukaemia Foundation of Australia and the Cure Cancer Australia Foundation, and an Early Career Fellowship from the Cancer Institute NSW. R.B. Lock is supported by a Fellowship from the National Health and Medical Research Council.

The costs of publication of this article were defrayed in part by the payment of page charges. This article must therefore be hereby marked *advertisement* in accordance with 18 U.S.C. Section 1734 solely to indicate this fact.

Received January 31, 2014; revised June 10, 2014; accepted June 29, 2014; published OnlineFirst July 10, 2014.

References

1. Hunger SP, Lu X, Devidas M, Camitta BM, Gaynon PS, Winick NJ, et al. Improved survival for children and adolescents with acute lymphoblastic leukemia between 1990 and 2005: a report from the children's oncology group. J Clin Oncol 2012;30:1663–9.
2. Ko RH, Ji L, Barnette P, Bostrom B, Hutchinson R, Raetz E, et al. Outcome of patients treated for relapsed or refractory acute lymphoblastic leukemia: a therapeutic advances in childhood leukemia consortium study. J Clin Oncol 2010;28:648–54.
3. Hanahan D, Weinberg RA. Hallmarks of cancer: the next generation. Cell 2011;144:646–74.
4. Cragg MS, Harris C, Strasser A, Scott CL. Unleashing the power of inhibitors of oncogenic kinases through BH3 mimetics. Nat Rev Cancer 2009;9:321–6.
5. Chen L, Willis SN, Wei A, Smith BJ, Fletcher JI, Hinds MG, et al. Differential targeting of prosurvival Bcl-2 proteins by their BH3-only ligands allows complementary apoptotic function. Mol Cell 2005;17:393–403.
6. Kelly PN, Strasser A. The role of Bcl-2 and its pro-survival relatives in tumourigenesis and cancer therapy. Cell Death Differ 2011;18:1414–24.
7. Oltersdorf T, Elmore SW, Shoemaker AR, Armstrong RC, Augeri DJ, Belli BA, et al. An inhibitor of Bcl-2 family proteins induces regression of solid tumours. Nature 2005;435:677–81.
8. Tse C, Shoemaker AR, Adickes J, Anderson MG, Chen J, Jin S, et al. ABT-263: a potent and orally bioavailable Bcl-2 family inhibitor. Cancer Res 2008;68:3421–8.
9. High LM, Szymanska B, Wilczynska-Kalak U, Barber N, O'Brien R, Khaw SL, et al. The Bcl-2 homology domain 3 mimetic ABT-737 targets the apoptotic machinery in acute lymphoblastic leukemia resulting in synergistic in vitro and in vivo interactions with established drugs. Mol Pharmacol 2010;77:483–94.
10. Lock R, Carol H, Houghton PJ, Morton CL, Kolb EA, Gorlick R, et al. Initial testing (stage 1) of the BH3 mimetic ABT-263 by the pediatric preclinical testing program. Pediatr Blood Cancer 2008;50:1181–9.
11. Gandhi L, Camidge DR, Ribeiro de Oliveira M, Bonomi P, Gandara D, Khaira D, et al. Phase I study of Navitoclax (ABT-263), a novel Bcl-2 family inhibitor, in patients with small-cell lung cancer and other solid tumors. J Clin Oncol 2011;29:909–16.
12. Wilson WH, O'Connor OA, Czuczman MS, LaCasce AS, Gerecitano JF, Leonard JP, et al. Navitoclax, a targeted high-affinity inhibitor of BCL-2, in lymphoid malignancies: a phase 1 dose-escalation study of safety, pharmacokinetics, pharmacodynamics, and antitumour activity. Lancet Oncol 2010;11:1149–59.
13. Rudin CM, Hann CL, Garon EB, Ribeiro de Oliveira M, Bonomi PD, Camidge DR, et al. Phase II study of single-agent navitoclax (ABT-263) and biomarker correlates in patients with relapsed small cell lung cancer. Clin Cancer Res 2012;18:3163–9.
14. Doi K, Li R, Sung SS, Wu H, Liu Y, Manieri W, et al. Discovery of marinopyrrole A (maritoclax) as a selective Mcl-1 antagonist that overcomes ABT-737 resistance by binding to and targeting Mcl-1 for proteasomal degradation. J Biol Chem 2012;287:10224–35.
15. Merino D, Khaw SL, Glaser SP, Anderson DJ, Belmont LD, Wong C, et al. Bcl-2, Bcl-x(L), and Bcl-w are not equivalent targets of ABT-737 and navitoclax (ABT-263) in lymphoid and leukemic cells. Blood 2012;119:5807–16.
16. van Delft MF, Wei AH, Mason KD, Vandenberg CJ, Chen L, Czabotar PE, et al. The BH3 mimetic ABT-737 targets selective Bcl-2 proteins

and efficiently induces apoptosis via Bak/Bax if Mcl-1 is neutralized. Cancer Cell 2006;10:389–99.
17. Yamaguchi R, Janssen E, Perkins G, Ellisman M, Kitada S, Reed JC. Efficient elimination of cancer cells by deoxyglucose-ABT-263/737 combination therapy. PLoS ONE 2011;6:e24102.
18. Yamaguchi R, Perkins G. Mcl-1 levels need not be lowered for cells to be sensitized for ABT-263/737-induced apoptosis. Cell Death Diff 2011;2:e227.
19. Certo M, Del Gaizo Moore V, Nishino M, Wei G, Korsmeyer S, Armstrong SA, et al. Mitochondria primed by death signals determine cellular addiction to antiapoptotic BCL-2 family members. Cancer Cell 2006;9:351–65.
20. Ni Chonghaile T, Sarosiek KA, Vo TT, Ryan JA, Tammareddi A, Moore Vdel G, et al. Pretreatment mitochondrial priming correlates with clinical response to cytotoxic chemotherapy. Science 2011;334: 1129–33.
21. Houghton PJ, Morton CL, Tucker C, Payne D, Favours E, Cole C, et al. The pediatric preclinical testing program: description of models and early testing results. Pediatr Blood Cancer 2007;49:928–40.
22. Liem NL, Papa RA, Milross CG, Schmid MA, Tajbakhsh M, Choi S, et al. Characterization of childhood acute lymphoblastic leukemia xenograft models for the preclinical evaluation of new therapies. Blood 2004; 103:3905–14.
23. Houghton PJ, Morton CL, Gorlick R, Lock RB, Carol H, Reynolds CP, et al. Stage 2 combination testing of rapamycin with cytotoxic agents by the Pediatric Preclinical Testing Program. Mol Cancer Ther 2010;9:101–12.
24. Rose WC, Wild R. Therapeutic synergy of oral taxane BMS-275183 and cetuximab versus human tumor xenografts. Clin Cancer Res 2004;10:7413–7.
25. Bachmann PS, Gorman R, Papa RA, Bardell JE, Ford J, Kees UR, et al. Divergent mechanisms of glucocorticoid resistance in experimental models of pediatric acute lymphoblastic leukemia. Cancer Res 2007;67:4482–90.
26. Bhadri VA, Cowley MJ, Kaplan W, Trahair TN, Lock RB. Evaluation of the NOD/SCID xenograft model for glucocorticoid-regulated gene expression in childhood B-cell precursor acute lymphoblastic leukemia. BMC Genomics 2011;12:565.
27. Benjamini Y, Hochberg Y. Controlling the false discovery rate: a practical and powerful approach to multiple testing. J R Statist Soc 1995;57:289–300.
28. Smyth GK. Linear models and empirical bayes methods for assessing differential expression in microarray experiments. Stat Appl Genet Mol Biol 2004;3:Article3.
29. Bonapace L, Bornhauser BC, Schmitz M, Cario G, Ziegler U, Niggli FK, et al. Induction of autophagy-dependent necroptosis is required for childhood acute lymphoblastic leukemia cells to overcome glucocorticoid resistance. J Clin Invest 2010;120:1310–23.
30. Coustan-Smith E, Mullighan CG, Onciu M, Behm FG, Raimondi SC, Pei D, et al. Early T-cell precursor leukaemia: a subtype of very high-risk acute lymphoblastic leukaemia. Lancet Oncol 2009;10:147–56.
31. Lock RB, Liem N, Farnsworth ML, Milross CG, Xue C, Tajbakhsh M, et al. The nonobese diabetic/severe combined immunodeficient (NOD/SCID) mouse model of childhood acute lymphoblastic leukemia reveals intrinsic differences in biologic characteristics at diagnosis and relapse. Blood 2002;99:4100–8.
32. Armstrong SA, Staunton JE, Silverman LB, Pieters R, den Boer ML, Minden MD, et al. MLL translocations specify a distinct gene expression profile that distinguishes a unique leukemia. Nat Genet 2002;30:41–7.
33. Nordlund J, Kiialainen A, Karlberg O, Berglund EC, Goransson-Kultima H, Sonderkaer M, et al. Digital gene expression profiling of primary acute lymphoblastic leukemia cells. Leukemia 2012;26:1218–27.
34. Szymanska B, Wilczynska-Kalak U, Kang MH, Liem NL, Carol H, Boehm I, et al. Pharmacokinetic modeling of an induction regimen for *in vivo* combined testing of novel drugs against pediatric acute lymphoblastic leukemia xenografts. PLoS ONE 2012;7:e33894.
35. Anderson K, Lutz C, van Delft FW, Bateman CM, Guo Y, Colman SM, et al. Genetic variegation of clonal architecture and propagating cells in leukaemia. Nature 2011;469:356–61.
36. Clappier E, Gerby B, Sigaux F, Delord M, Touzri F, Hernandez L, et al. Clonal selection in xenografted human T cell acute lymphoblastic leukemia recapitulates gain of malignancy at relapse. J Exp Med 2011;208:653–61.
37. Schmitz M, Breithaupt P, Scheidegger N, Cario G, Bonapace L, Meissner B, et al. Xenografts of highly resistant leukemia recapitulate the clonal composition of the leukemogenic compartment. Blood 2011;118:1854–64.
38. Tahir SK, Wass J, Joseph MK, Devanarayan V, Hessler P, Zhang H, et al. Identification of expression signatures predictive of sensitivity to the Bcl-2 family member inhibitor ABT-263 in small cell lung carcinoma and leukemia/lymphoma cell lines. Mol Cancer Ther 2010;9:545–57.
39. Maurer U, Charvet C, Wagman AS, Dejardin E, Green DR. Glycogen synthase kinase-3 regulates mitochondrial outer membrane permeabilization and apoptosis by destabilization of MCL-1. Mol Cell 2006;21:749–60.
40. Nijhawan D, Fang M, Traer E, Zhong Q, Gao W, Du F, et al. Elimination of Mcl-1 is required for the initiation of apoptosis following ultraviolet irradiation. Genes Dev 2003;17:1475–86.
41. Gao Y, Koide K. Chemical perturbation of Mcl-1 pre-mRNA splicing to induce apoptosis in cancer cells. ACS Chem Biol 2013;8: 895–900.
42. Boiani M, Daniel C, Liu X, Hogarty MD, Marnett LJ. The stress protein BAG3 stabilizes Mcl-1 protein and promotes survival of cancer cells and resistance to antagonist ABT-737. J Biol Chem 2013;288:6980–90.
43. Manabe A, Coustan-Smith E, Behm FG, Raimondi SC, Campana D. Bone marrow-derived stromal cells prevent apoptotic cell death in B-lineage acute lymphoblastic leukemia. Blood 1992;79:2370–7.
44. Klumper E, Pieters R, Veerman AJP, Huismans DR, Loonen AH, Hahlen K, et al. In vitro cellular drug resistance in children with relapsed/refractory acute lymphoblastic leukemia. Blood 1995;86:3861–8.
45. Kumagai M, Manabe A, Pui C-H, Behm FG, Raimondi SC, Hancock ML, et al. Stroma-supported culture of childhood B-lineage acute lymphoblastic leukaemia cells predicts treatment outcome. J Clin Invest 1996;97:755–60.
46. Pieters R, Loonen AH, Huismans DR, Broekema GJ, Dirven MWJ, Heyenbrok MW, et al. *In vitro* drug sensitivity of cells from children with leukemia using the MTT assay with improved culture conditions. Blood 1990;76:2327–36.
47. Ackler S, Mitten MJ, Foster K, Oleksijew A, Refici M, Tahir SK, et al. The Bcl-2 inhibitor ABT-263 enhances the response of multiple chemotherapeutic regimens in hematologic tumors *in vivo*. Cancer Chemother Pharmacol 2010;66:869–80.
48. Kang MH, Kang YH, Szymanska B, Wilczynska-Kalak U, Sheard MA, Harned TM, et al. Activity of vincristine, L-ASP, and dexamethasone against acute lymphoblastic leukemia is enhanced by the BH3-mimetic ABT-737 in vitro and in vivo. Blood 2007;110:2057–66.
49. Souers AJ, Leverson JD, Boghaert ER, Ackler SL, Catron ND, Chen J, et al. ABT-199, a potent and selective BCL-2 inhibitor, achieves antitumor activity while sparing platelets. Nat Med 2013; 19:202–8.
50. Vandenberg CJ, Cory S. ABT-199, a new Bcl-2-specific BH3 mimetic, has *in vivo* efficacy against aggressive Myc-driven mouse lymphomas without provoking thrombocytopenia. Blood 2013;121:2285–8.